Part III

Flow and dissipation

Cambridge University Press
978-0-521-70524-0 - Advanced Magnetohydrodynamics: With Applications to Laboratory and Astrophysical Plasmas
J. P. (Hans) Goedbloed, Rony Keppens and Stefaan Poedts
Excerpt
More information

12

Waves and instabilities of stationary plasmas

12.1 Laboratory and astrophysical plasmas

12.1.1 Grand vision: magnetized plasma on all scales

In Chapter 1 of the preceding Volume [1] we pointed out that, since more than 90% of visible matter in the Universe is plasma, the dynamics of plasmas and the associated magnetic fields are an important constituent of the description of nature. In Chapter 4 [1], we then showed that *the equations of magnetohydrodynamics (MHD) are scale-independent*: the scales of length, density and magnetic field strength of a magnetically confined plasma may be divided out. This simple fact has the amazing consequence that the macroscopic dynamics of plasmas in both laboratory fusion devices (tokamaks, stellarators, etc.) and astrophysical objects (stellar coronae, accretion disks, spiral arms of galaxies, etc.) may be described by the same equations, viz. the equations of MHD. We encountered several examples of this before, in Volume [1]. In the present Volume [2], we will continue the investigation of this common field of research by means of the new "wide-angle MHD telescope".

Figure 12.1 shows two representative, but very different, examples from science and technology, viz. the design drawing of the international tokamak experimental reactor ITER, presently under construction, and an image made by the Hubble Space Telescope of the Pinwheel Galaxy M101. The consequence of scale-independence is that the most obvious difference of the two configurations, their length scale indicated next to the figure, is actually irrelevant for the description of macroscopic plasma dynamics!

▷ **Scale-dependent models** To avoid misunderstanding: small-scale kinetic or two-fluid effects like electron inertia [20], described by the scale-dependent model of Hall-MHD, can have macroscopic consequences like reconnection and waves (see Section 14.5), which may even be detectable by spacecrafts flying through the bow shock of the magnetosphere; see Stasiewicz [418]. Likewise, in the description of hot plasmas in thermonuclear confinement experiments, kinetic effects exhibit a bewildering range of dynamical phenomena on many spatial and temporal scales presenting a challenge to the computational modeling of these plasmas by different, scale-dependent, fluid closures; see Schnack *et al.* [403]. ◃

For our present purpose, the Hubble Space Telescope picture is somewhat misleading since it only shows the stars and dust. Roughly an equal amount of plasma should be present in the plasma component of galaxies (not counting the plasma interiors of the stars themselves), and much more mass should be present in the dark matter component. According to a recent review by Fukugita [150], for the Universe as a whole the balance is shifted significantly towards plasma: ten times more mass is present in plasmas than in stars (again, not counting the fact that stars themselves are mostly plasma). Since we have no clue about the physics of dark matter, it might be advisable to first investigate the plasma component with all techniques that are presently available. Recalling our critical discussion of the standard view of nature, which does not articulate the distinction between neutral gas and plasma, as schematically represented in Figure 1.8 [1], one would expect on the contrary that the abundance of plasma ($\equiv$ abundance of magnetic fields $\equiv$ global anisotropic dynamics) should play a much more prominent role in the description of the Universe than it has done up till now.

In fact, there are many signs that astrophysics is beginning to fill in this gap. For example, when Land and Magueijo [292] established that there is a small but statistically significant anisotropy, with a preferred axis, in the cosmic background radiation as observed with the WMAP satellite, the far-going implications for cosmology were immediately realized. A number of researchers, e.g. Hutsemékers [234] and Longo [316], started to speculate that, amongst other more exotic possibilities, a large-scale cosmic magnetic field might be involved.

As another example, Kaastra *et al.* [251], and several other researchers (see the review by Peterson and Fabian [368]), have recently pointed out that magnetic fields may play an important role in the dynamics of clusters of galaxies. From X-ray spectra obtained from the XMM-Newton satellite, they conclude that magnetized plasmas in huge magnetic loops, of similar spatial structure to those in stellar coronae, may be responsible for the temperature decrement observed for cooling plasma flows in those clusters.

Also, recently, filaments of warm hot intergalactic matter (WHIM) connecting clusters of galaxies have been detected unequivocally by Werner *et al.* [478] by means of X-ray images obtained from the same satellite. This discovery appears to agree with dark matter simulations that ascribe this “cosmic web” mainly to dark matter, but it would come as no surprise if the filamentary structure were associated with a magnetized plasma component as well. The bookkeeping of the gravitational effects ascribed to dark matter might well change in the direction of a larger contribution of plasma.

Whatever the final outcome of these debates will be, it is probable that plasma

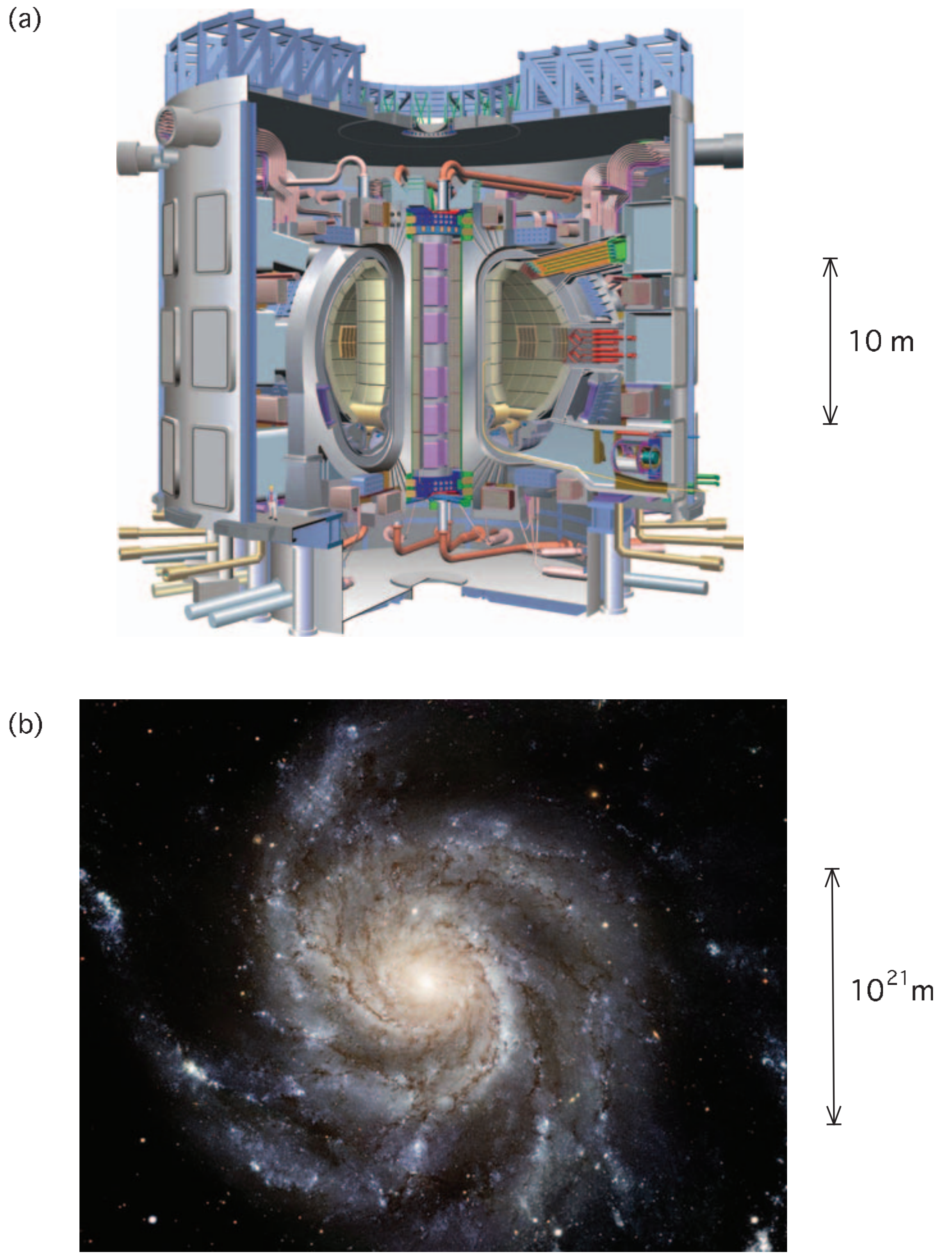

Fig. 12.1 Magnetized plasmas in the laboratory and in astrophysics: (a) the international tokamak experimental reactor ITER; (b) the Pinwheel Galaxy M101 (HST, NASA-ESA).

and, hence, magnetic fields will become much more central for our understanding of the dynamics of the Universe at large than presently accounted for.

12.1.2 Differences between laboratory and astrophysical plasmas

Although scale-independence of the MHD equations permits analysis of global plasma dynamics in laboratory and astrophysical plasmas by the same techniques, the important differences of the parameters that govern overall force balance should not be lost sight of. For example, the parameter $\beta \equiv 2\mu_0 p/B^2$ is small for tokamak plasmas and usually large for astrophysical plasmas, so that plasma dynamics in tokamaks is always dominated by magnetic fields whereas this may not be the case for astrophysical plasmas.

Roughly speaking, one could distinguish the two kinds of plasma configurations on the basis of the following global equilibrium characteristics.

(a) Tokamaks are *magneto*-hydrodynamic plasmas, with a magnetic field that is approximately a force-free field (FFF),

$$\begin{aligned} \mathbf{j}\times\mathbf{B} &\approx 0 \qquad \textit{(FFF to leading order)} \\ &= \nabla p \ \sim \beta \ll 1 \qquad \textit{(important correction)}\,. \end{aligned} \tag{12.1}$$

Consequently, the equilibrium is nearly exclusively determined by the magnetic field geometry, but the pressure corrections are essential since they determine the power output of a future fusion reactor.

(b) Most astrophysical objects are *hydro*-magnetic plasmas, with sizeable flows, and the gravitational acceleration is usually not negligible,

$$\begin{aligned} \rho\mathbf{v}\cdot\nabla\mathbf{v} + \nabla p + \rho\nabla\Phi &\approx 0 \qquad \textit{(Keplerian flow to leading order)} \\ &= \mathbf{j}\times\mathbf{B} \ \sim \beta^{-1} \ll 1 \quad \textit{(important correction)}\,. \end{aligned} \tag{12.2}$$

Consequently, gravity and rotation usually dominate over the magnetic terms, but the latter may be crucial for the growth or damping of instabilities (as for the Parker instability, discussed below, and the magneto-rotational instability which even operates when the magnetic field is infinitesimal, see Section 13.4.2).

It is well known that a force-free magnetic field cannot be extended indefinitely, as follows from the virial theorem (see Shafranov [409], p. 106). Eventually, the magnetic pressure has to be balanced by something. In tokamaks, equilibrium is due to balancing of the Lorentz forces on the plasma by mechanical forces on the induction coils, which have to be firmly fixed to the laboratory by "nuts and bolts". (Without those, the configuration would simply fly apart: a magnetic field of $5\,\mathrm{T}$ exerts a pressure of $B^2/(2\mu_0) \approx 10^7\,\mathrm{N\,m^{-2}} \approx 100\,\mathrm{atm.}$) The mechanical counterpart for accretion disks or galaxies is balancing of the centrifugal acceleration by the gravitational pull of the central objects, which may include a black hole. The implications of this difference for stability are much more wide-ranging than generally realized, as will be illustrated by contrasting "intuition" developed on tokamak stability to some major instabilities operating in astrophysical plasmas.

Interchanges in tokamaks and Parker instability in galaxies

To appreciate the issue, let us pronounce some general features of tokamak stability theory, based on the results from the quasi-cylindrical approximation presented in Section 9.4 [1] and anticipating the exact toroidal representation to be developed in Chapter 17. For the present purpose, the difference between the cylindrical approximation in terms of r, θ and z and the toroidal representation in terms of ψ (the poloidal magnetic flux, the "radial" coordinate), ϑ (the poloidal angle) and φ (the toroidal angle) may be ignored. Without exaggeration, it may then be said that the wide variety of MHD instabilities operating in tokamaks, represented by normal modes of the form

$$f(\psi, \vartheta, \varphi, t) = \textstyle\sum_m \widetilde{f}_m(\psi)\, \mathrm{e}^{\mathrm{i}(m\vartheta + n\varphi - \omega t)} , \tag{12.3}$$

is unstable only for (approximately) perpendicular wave vectors,

$$\mathbf{k}_0 \perp \mathbf{B} \quad \Rightarrow \quad -\mathrm{i}\mathbf{B}\cdot\nabla \sim m + nq \approx 0 . \tag{12.4}$$

The reason is the enormous field line bending energy of the Alfvén waves,

$$W_\mathrm{A} \approx \tfrac{1}{2} \int \Big[(\mathbf{k}_0 \cdot \mathbf{B})^2 \, |\mathbf{n}\cdot\boldsymbol{\xi}|^2 + \cdots \Big] \, dV \gg 0 , \tag{12.5}$$

so that field line localization ($k_\parallel \ll k_\perp$) is necessary to eliminate this term and to get instability from the different higher order terms due to, e.g. pressure gradients and currents. The Ansatz (12.4) is made in virtually all tokamak stability calculations, like in the derivation of the Mercier criterion [331] involving *interchanges* on rational magnetic surfaces, of *ballooning modes* [91] involving localization about rational magnetic field lines, of *internal kink modes*, of *neo-classical tearing modes*, of *external kink modes*, etc.; see Sections 17.2 and 17.3. All involve localization about rational magnetic surfaces, either inside the plasma or in an outer vacuum. Hence, it became a kind of "intuition" in tokamak physics to assume that this is a general truth about plasma instabilities.

In contrast, some major instabilities in astrophysical plasmas turn out to operate under precisely the opposite conditions:

$$\mathbf{k}_0 \parallel \mathbf{B} \quad \Rightarrow \quad -\mathrm{i}\mathbf{B}\cdot\nabla \sim m + nq \approx 1 . \tag{12.6}$$

These include the *Parker instability* operating in spiral arms of galaxies [365] and the *magneto-rotational instability* [467, 83, 18] which is held responsible for the turbulent dissipation in accretion disks about a compact object. Both have their largest growth rates when the wave vector $\mathbf{k}_0$ is about parallel to the magnetic field, and certainly not perpendicular! (It is most peculiar that this apparent contradiction with stability of laboratory plasmas went unnoticed so far.) How is the above argument about the dominance of field line bending energy circumvented for astrophysical plasmas?

In order to answer that question, let us compare how the two entirely different pairs of equilibrium conditions (12.1) and (12.2), and the associated pairs of instability conditions (12.4) and (12.6), appear in the analysis of the gravitational interchange [171]. This instability has played an important role in modeling both the stability of laboratory plasmas (where gravity is used as just a way to simulate magnetic field line curvature) and the Parker instability [365] which is concerned with instability due to genuine gravity in spiral arms of galaxies.

To that end, we recapitulate the major conclusions on the gravitational interchange from Sections 7.5.2 and 7.5.3 [1], Eqs. (7.199), (7.206) and (7.212). The stability criterion for gravitational interchanges of a plane plasma slab reads:

$$-\rho N_{\mathrm{B}}^2 \equiv \rho' g + \frac{\rho^2 g^2}{\gamma p} \le \tfrac{1}{4} B^2 \varphi'^2 \,, \tag{12.7}$$

where N_{B} is the Brunt–Väisäläa frequency and φ' is the magnetic shear. Without magnetic shear, stability just appears to depend on the square of the Brunt–Väisäläa frequency: $N_{\mathrm{B}}^2 \ge 0$, which amounts to the Schwarzschild criterion for convective stability when expressed in terms of the equilibrium temperature gradient. This criterion is obtained from the marginal equation of motion ($\omega^2 = 0$) in the limit of small parallel wave number ($k_\parallel \to 0$). However, when these two limits are interchanged ($k_\parallel = 0$ and $\omega^2 \to 0$), an entirely different criterion is obtained:

$$-\rho N_{\mathrm{M}}^2 \equiv \rho' g + \frac{\rho^2 g^2}{\gamma p + B^2} \le 0 \,, \tag{12.8}$$

where N_{M} is the magnetically modified Brunt–Väisäläa frequency. The apparent discrepancy between these stability criteria was resolved by Newcomb [348] who noted that there is a cross-over of two branches of the local dispersion equation with the solutions

$$\omega_1^2 = (k_0^2/k_{\mathrm{eff}}^2)\, N_{\mathrm{M}}^2 \qquad \textit{(pure interchanges)}\,, \tag{12.9}$$

$$\omega_2^2 = \frac{N_{\mathrm{B}}^2}{N_{\mathrm{M}}^2}\,\frac{\gamma p}{\gamma p + B^2}\,\frac{1}{\rho}\,(\mathbf{k}_0\cdot\mathbf{B})^2 \qquad \textit{(quasi-interchanges)}\,, \tag{12.10}$$

where the last mode is the first to become unstable when the density gradient is increased. The first expression holds for $k_\parallel = 0$, where the factor $k_{\mathrm{eff}}^2 \equiv k_0^2 + n^2\pi^2/a^2$ indicates clustering of the modes, $\omega_1^2 \to 0$, when the vertical mode number becomes large, $n \to \infty$ (this n should not be confused with the toroidal mode number n introduced above), and the second expression is only valid for $k_\parallel \ll k_\perp$. Hence, *field line bending is small in both cases.*

In cylindrical and toroidal plasmas, magnetic field line curvature is unavoidable and interchange instabilities then arise when the negative pressure gradient (associated with confinement) exceeds the shear of the magnetic field lines, analogous to the gravitational interchange criterion (12.7). This is expressed by the criteria of Suydam [427], Eq. (9.118) [1], and Mercier [331], Eq. (17.98). For cylindrical plasmas without magnetic shear, expressions were derived for the growth rates of interchanges and quasi-interchanges [474, 160, 177], analogous to Eqs. (12.9) and (12.10) with the following replacements:

$$N_{\rm M}^2 \rightarrow \frac{2B_\theta^2}{\rho r B^2}\Big(p' + \frac{\gamma p}{\gamma p + B^2}\frac{2B_\theta^2}{r}\Big)\,, \qquad N_{\rm B}^2 \rightarrow \frac{2B_\theta^2}{\rho r B^2}\, p'\,. \tag{12.11}$$

As illustrated in Figs. 9.15 and 9.11 [1], when p' becomes negative (violation of the shearless limit of Suydam's criterion) first the quasi-interchanges become unstable and the pure interchanges become unstable when $p' \leq -\gamma p\,(\gamma p + B^2)^{-1}\,(2B_\theta^2)/r$, in agreement with the expression for the z-pinch derived by Kadomtsev [252].

It would appear that the analogy between plasmas with curved magnetic fields and gravitational plasmas is perfect: instability only occurs at the interchange value $k_\parallel = 0$ or close to it. However (we now complete the analysis of the gravito-MHD waves started in Section 7.3.3 [1]), the *Parker instability* operates under precisely opposite conditions ($k_\perp \approx 0$). For an exponential atmosphere, its growth rate is given by expanding the expression (7.112) [1]:

$$\omega^2 \approx \Big(1 + \frac{\rho N_{\rm B}^2}{k_{\rm eff}^2 B^2}\Big)\, \frac{\gamma p}{\gamma p + B^2}\, \frac{1}{\rho}\,(k_0 B)^2\,. \tag{12.12}$$

This looks similar to the expression (12.10) for the quasi-interchanges, which gives the growth rate at $k_\parallel \approx 0$ for *localized modes* ($n \rightarrow \infty$), but it is actually completely different since the expression (12.12) for the Parker instability requires $k_\perp \approx 0$ and only yields instability for *global modes* ($n \approx 1$). This is so because the criterion for the Parker instability, $k_{\rm eff}^2 B^2 + \rho N_{\rm B}^2 < 0$, cannot be satisfied for $n \rightarrow \infty$, since $k_{\rm eff} \rightarrow \infty$ then. In other words, it is very well possible to have a global instability when the field line bending energy (12.5) is not small at all! This is also the case for the magneto-rotational instability (see Section 13.4.2).

Hence, MHD instabilities occur in astrophysical plasmas under conditions that do not allow instability in laboratory plasmas. The reason is the stabilizing "backbone" of a large toroidal magnetic field in the latter. Estimating orders of magnitudes for an equilibrium with inhomogeneity length scale L, the Parker instability requires

$$N_{\rm B}^2 \sim -\frac{B^2}{\rho L^2}\,, \quad \text{with} \quad \beta \sim 1\,. \tag{12.13}$$

(Note that a sizeable magnetic field is required, actually violating the simplified order of magnitude estimate $\beta \gg 1$ of Eq. (12.2)(b).) In contrast, the corresponding term of Eq. (12.11)(b) for curvature–pressure gradient driven interchanges in quasi-cylindrical/toroidal equilibria requires

$$\frac{2B_\theta^2}{\rho r B^2}\, p' \sim -\epsilon^2 \beta \cdot \frac{B^2}{\rho L^2}\,, \quad \text{with } \epsilon \equiv a/R_0 \ll 1\,, \ \ \beta \sim \epsilon^2\,. \tag{12.14}$$

In the first case, the driving force of the instability can compete with the field line bending contributions (12.5). In the latter case, because of the small factor $\epsilon^2\beta \sim \epsilon^4$, this is impossible so that pressure-driven interchanges in cylindrical and toroidal plasmas never occur for $\mathbf{k}_0 \parallel \mathbf{B}$. Consequently, tokamak "intuition" focusing on rational magnetic surfaces and field lines as exclusively determining stability may be misleading for astrophysical plasmas.

The two different view points can be reconciled as follows. Whereas the condition (12.4) for tokamak instability automatically leads to study of the degeneracy and couplings of the Alfvén and slow continua close to marginal stability ($\omega \approx 0$), an entirely different path to avoid the stabilizing contribution (12.5) of the Alfvén waves is exploited by the Parker instabilities. These are actually modified slow magneto-acoustic waves avoiding the coupling to the Alfvén waves by remaining orthogonal to them: the polarization (expressed by the eigenvector $\boldsymbol{\xi}$) of the Parker (slow) modes is parallel to $\mathbf{B}$ (flow along the magnetic field is essential), whereas the polarization of the Alfvén waves is mainly perpendicular to $\mathbf{B}$. This orthogonality is clearly exhibited by Fig. 12.2, which shows the complete low-frequency part of the spectrum of modes for a gravitating plasma slab with exponential dependence on height of the density, magnetic field and pressure, for different values of the angle ϑ between the horizontal wave vector $\mathbf{k}_0$ and the magnetic field.

The exponentially stratified equilibrium was analyzed in Section 7.3.2 [1], resulting in the dispersion equation (7.116) with solutions shown in Fig. 7.10 for fixed angle ϑ. These solutions are now shown in Fig. 12.2(a) for all directions of $\mathbf{k}_0$. At $\vartheta = 0$ ($\mathbf{k}_0 \parallel \mathbf{B}_0$), the Parker instability has its largest growth rate, whereas around $\vartheta = \frac{1}{2}\pi$ ($\mathbf{k}_0 \perp \mathbf{B}_0$), the interchanges and quasi-interchanges operate. These two ranges correspond to two different instability mechanisms: in the $k_\parallel \approx 0$ range, coupling of *local* (high n) slow and Alfvén modes causes interchange or quasi-interchange instability, whereas in the range $k_\perp \approx 0$, *global* (low n) instability of the slow magneto-sonic branch, viz. the Parker instability, occurs. In the intermediate range, there is a smooth transformation from the Parker instability to interchanges via modes that we have termed *quasi-Parker instabilities*.

The local interchange and quasi-interchange instabilities are modified substantially by the introduction of magnetic shear,

$$\mathbf{B} = B_0 \mathrm{e}^{-\frac{1}{2}\alpha x}\,[\,\sin(\lambda x)\mathbf{e}_y + \cos(\lambda x)\mathbf{e}_z]\,. \tag{12.15}$$

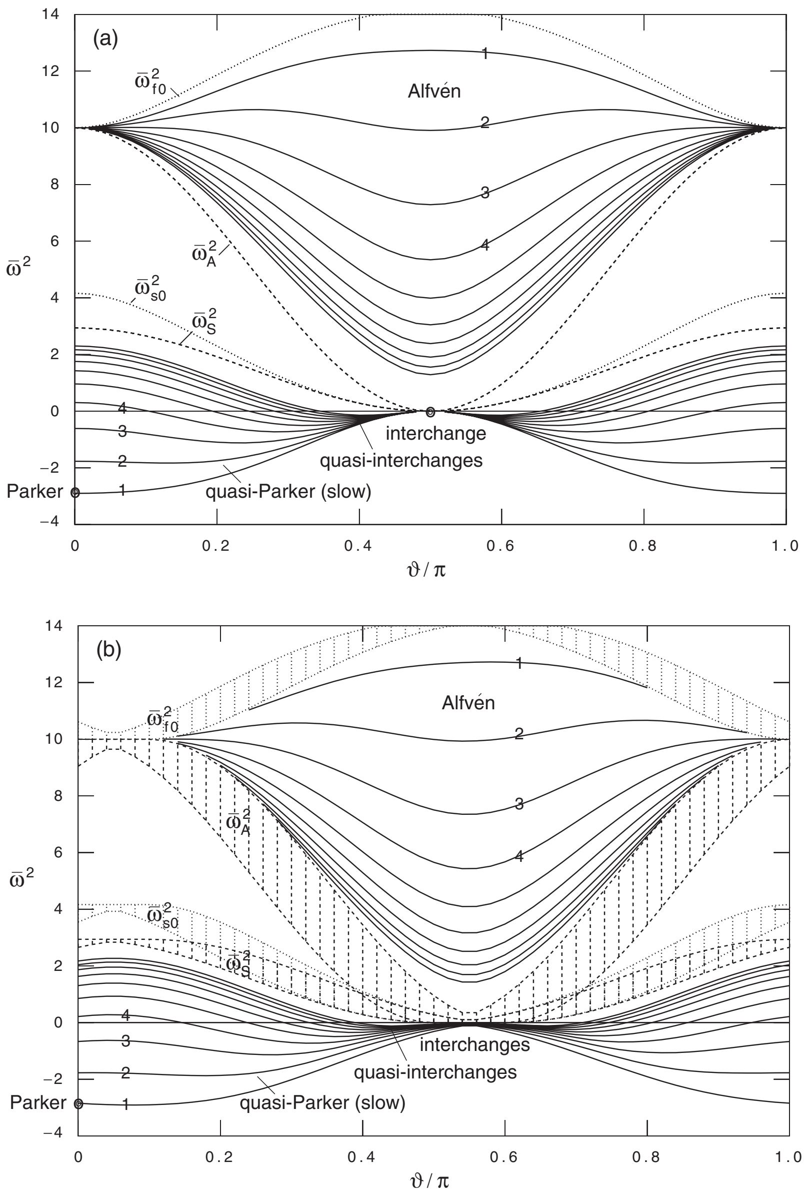

Fig. 12.2 Spectrum of slow (quasi-Parker) instabilities, connecting the Parker instability to the quasi-interchanges, and Alfvén waves for different angles between $\mathbf{k}_0$ and $\mathbf{B}_0$ for exponential atmosphere with (a) uni-directional field ($\bar{\lambda} = 0$), (b) magnetic shear ($\bar{\lambda} = 0.3$) and genuine continua $\bar{\omega}^2_{\rm A}$ and $\bar{\omega}^2_{\rm S}$; $\bar{\alpha} = 20$, $\beta = 0.5$, $\bar{k}^2_0 = 10$, $\bar{q} = n\pi$ $(n = 1, 2, \ldots, 10)$.

Except for modifying the stability properties, it also leads to the bands of continuous spectra $\omega^2_{\rm A}$ and $\omega^2_{\rm S}$ separating the Alfvén waves from the gravitational insta-